The physics of CO2 transfer during carbonated water injection into oil reservoirs: From non-equilibrium core-scale physics to field-scale implication

Accepted Manuscript

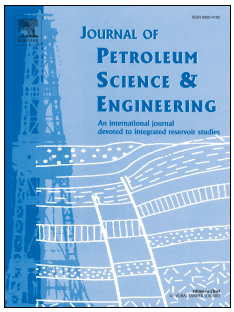

The physics of CO_2 transfer during carbonated water injection into oil reservoirs: From non-equilibrium core-scale physics to field-scale implication

Jalal Foroozesh, Mahmoud Jamiolahmady

PII: S0920-4105(18)30275-4

DOI: 10.1016/j.petrol.2018.03.089

Reference: PETROL 4830

To appear in: *Journal of Petroleum Science and Engineering*

Received Date: 20 November 2017

Revised Date: 2 February 2018

Accepted Date: 26 March 2018

Please cite this article as: Foroozesh, J., Jamiolahmady, M., The physics of CO_2 transfer during carbonated water injection into oil reservoirs: From non-equilibrium core-scale physics to field-scale implication, *Journal of Petroleum Science and Engineering* (2018), doi: 10.1016/j.petrol.2018.03.089.

Graphical Abstract

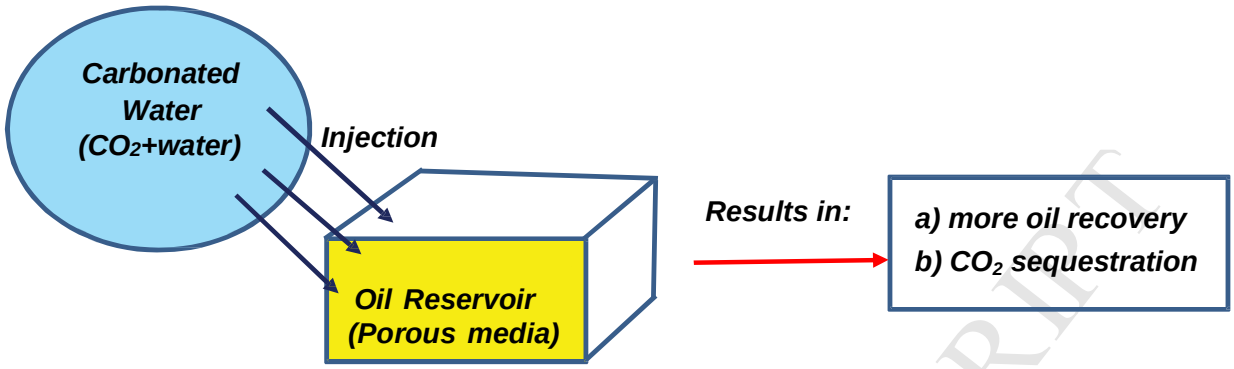

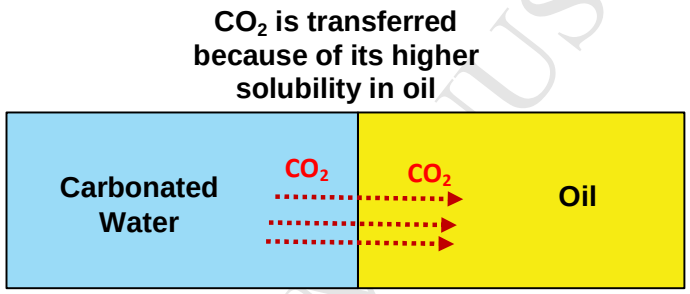

Question: **Is the CO_2 transfer quick or slow? Can we reach equilibrium state during this process?**

Answer: ***If Equilibrium Number, N_e= L MTC A /q_{inj}, is greater than 0.2 the system can reach the equilibrium state during CWI process that is true at large scale.***

The physics of CO_2 transfer during carbonated water injection into oil reservoirs: From non-equilibrium core-scale physics to field-scale implication

Jalal Foroozesh[a*], Mahmoud Jamiolahmady[b]

[a]: Universiti Teknologi PETRONAS, Petroleum Engineering Department, Perak, Malaysia

[b]: Heriot-Watt University, Institute of Petroleum Engineering, Edinburgh, UK

*Corresponding author:

Email: jalal.foroozesh@gmail.com, jalal.foroozesh@utp.edu.my

ABSTRACT

CO_2 can be dissolved into water to make carbonated water (CW). CW can be injected into oil reservoirs for enhanced oil recovery (EOR) and CO_2 sequestration purposes. Carbonated water injection (CWI) technique is a cost-effective CO_2 based injection strategy that needs less amount of CO_2 as compared to other CO_2-EOR techniques. We previously showed that for simulation of CWI coreflood experiments, the kinetics of CO_2 transfer between the phases should be considered and we accordingly developed a non-equilibrium based two-phase compositional simulator. We also used the developed simulator to simulate some CWI coreflood experiments. This paper aims to explore the role of mass transfer during simulation of CWI process at field (large)-scale by analysing the data of core-scale simulations. To do so, the results of CWI core-scale simulations obtained from our non-equilibrium based simulator are benchmarked against the results from an equilibrium based simulator and a dimensionless number so-called equilibrium number (N_e) is introduced. It is shown that in a specific range of N_e values, the contact time of the phases inside the system is large enough that the CO_2 can be distributed between the phases based on its equilibrium concentration. Contrary to core-scale simulation, it is concluded that mass transfer kinetics during large-

scale simulation of CWI process is not important. Moreover, higher oil recovery factor and CO_2 storage are predicted at large-scale (reservoir-scale) as compared to the core-scale's results. The findings of this paper can help to better understand the importance of mass transfer kinetics between the phases in porous media.

Keywords: Carbonated water injection (CWI); Mass transfer; Equilibrium; CO_2 storage; Core-scale; Reservoir-scale

1. INTRODUCTION

CO_2 gas is injected into oil reservoirs with the objectives of enhancing oil recovery and also sequestration. CO_2 can be injected on its own (conventional CO_2 injection), together with water under WAG (water alternating gas) or through carbonated water injection (CWI) strategies. In CWI, CO_2 is dissolved in water before injection in order to improve the efficiency of conventional water injection (WI). That is, CWI can be considered as an improved WI process. Upon injection of carbonated water (CW) into an oil reservoir and when CW contacts oil in the reservoir, CO_2 migrates from water to the oil phase due to its higher solubility in hydrocarbons, improving the oil mobility. As a result, a higher oil recovery factor is expected. Comparing CWI and conventional CO_2 injection, CWI needs less volume of CO_2 and more importantly CO_2 is in the dissolved state (dissolved in oil or water phase) during the process which results in better sweep efficiency, less fingering issue and less risk of CO_2 leakage [1-3]. Numerous experimental studies on CWI can be found in the literature. The reported experimental studies include direct flow visualization using micromodel setup [4, 3, 5], coreflood experiments [6-10, 3] and also sand packed experiments [11, 12]. All the experimental reports confirm a better recovery factor by CW compared to that by WI, with the potential of CO_2 storage at end of the experiments. Depending on reservoir and fluid characteristics, the mechanisms contributing towards incremental recovery factor by CWI are: oil swelling, viscosity and IFT reduction and

wettability alteration [1, 2, 13, 4, 10, 3, 5]. On the other hand, solubility trapping [14, 15]) is the main CO_2 storage mechanism, as the CO_2 remains dissolved in residual oil and water fluids inside the reservoir at end of the process leading to long storage of CO_2 underground[2, 16, 10, 3].

There are not many comprehensive mathematical studies available on CWI as compared to experimental investigations. As reported in the literature, the conventional compositional simulation approach has been usually used to study CWI [6, 17]. In the compositional approach, it is inherently assumed that, CO_2 will be distributed between water and oil phase during CWI process based on the local equilibrium constraint that might not be a valid assumption as discussed in the literature. For instance, Kechut et al.[9] used ECLIPSE300 (E300) compositional simulator to simulate some CWI coreflood experiments and realized that the recovery factor was over predicted. They attributed this to the local equilibrium assumption made by E300 allowing more CO_2 transfer into the oil phase than actually occurred during the conducted coreflood experiments. Accordingly, we previously developed a new non-equilibrium based compositional simulator[1, 2] where the mass transfer kinetics was included. We studied some CWI coreflood experiments and showed that the equilibrium state had not been reached in the simulated CWI experiments as captured by our simulator. It has been mentioned in the literature that [18], the equilibrium might not be reached during gas flooding projects with relatively short contact time, that can be true for laboratory coreflood experiments. It should be noted that, during gas injection coreflood experiments, components can be transferred and exchanged between the gas and liquid phases while the convective flow time scale is usually larger than the mass transfer time scale due to high mobility of gas phase and short length of the core. As a result, the gas can leave the core quickly (gas breakthrough) without having enough contact time needed for mass exchange. That is, the system might not reach the equilibrium state due to short resident time[19]. Non-

equilibrium situation as a result of limited interphase mass transfer rate, has been studied widely by hydrologists and environmental engineers. Interphase mass transfer has been extensively considered by environmental scientists to study the dissolution rate of organic compounds from non-aqueous phase liquids (NAPL) trapped subsurface into groundwater [20-25]. Miller et al. (1990) investigated the equilibrium condition in a packed bed setup when the interphase mass transfer between flowing water and residual NAPL phases was studied. They observed that at a higher pore velocity, the interphase mass transfer rate is higher however, the retention time of fluids is lower resulting into a lower mass exchange and a non-equilibrium situation. In terms of the contact time, it is important to explain how large the contact time should be to reach the equilibrium. Dimensionless numbers (groups) can help to compare the importance of different physics based on the characteristics of the system under study. Dimensionless numbers can also help to easily compare the performance of various systems with different characteristics and scales. Zhou et al. (1997) defined three scaling groups (dimensionless numbers) to study multiphase flow in heterogeneous reservoirs when the boundaries between different flow regimes were determined based on the values of scaling groups [26]. Wood et al. (2008) introduced some dimensionless groups to describe the performance of CO_2 flooding mainly in Gulf Coast reservoirs by generating dimensionless oil recovery and CO_2 storage curves [27]. Li et al. (2015) developed some response functions by using some dimensionless groups (parameters) to estimate the maximum amount of CO_2 storage and oil recovery factor during CO_2 flooding into reservoirs with gravity effect and horizontal wells [28]. In their research, Li et al. (2015) used some known dimensionless parameters including residual hydrocarbon and water saturations, Buoyancy ratio and number, CO_2-oil and water-oil mobility ratios, and Dykstra–Parsons heterogeneity coefficient to explicitly relate the oil recovery factor and CO_2 storage efficiency to reservoir and fluid characteristics. The used Computer Modelling Groups'

CMG-GEM compositional simulator and ran a sensitivity analysis to find the effects of aforementioned dimensionless parameters on the recovery factor and CO_2 storage efficiency. However, they did not consider the mass transfer effect and assumed equilibrium conditions during CO_2 flood projects in their research. In our study here, we aim to investigate the role of mass transfer during CWI as a CO_2-EOR technique. In other words, the objective of this study is to identify the conditions at which we can assume the equilibrium is achieved during a CWI process. It is expected that, in the case of CWI coreflood experiments, if the CO_2 transfer rate from water into oil phase is large or equivalently if the contact time of water and oil in the core is long, the equilibrium state can be achieved. Therefore, it is important to be able to estimate the contact time that would ensure an equilibrium state. To reach this goal, we need to analyze the results of coreflood simulations using appropriate dimensionless numbers. In the following sections, we first present a summary of the structure of our non-equilibrium based simulator. Then we compare its core-scale simulation results with those of E300 commercial compositional simulator to identify the criteria needed for reaching an equilibrium state during coreflood experiments. Next we use the results of the core-scale simulation and scale them up to investigate CWI at reservoir-scale.

2. METHODOLOGY

To study the CWI process, we previously developed a two-phase (oil and water), 1-D model to capture a three-components system (oil, water and CO_2). The model was coded using MATLAB software and it solves numerically the following coupled partial differential equations (PDEs) based on fully implicit finite difference method [1, 2]. More details on numerical solution of the following PDEs are given in Appendix.

$$\frac{\partial}{\partial x}\left(\rho_O \frac{k\,Kr_O}{\mu_O}\frac{\partial p_O}{\partial x}\omega_{o-O}\right) = \varphi\frac{\partial(\rho_O s_O \omega_{o-O})}{\partial t} \tag{1a}$$

$$\frac{\partial}{\partial x}\left(\rho_O \frac{k\,Kr_O}{\mu_O}\frac{\partial p_O}{\partial x}\omega_{CO_2-O}\right) + U = \varphi\frac{\partial(\rho_O s_O \omega_{CO_2-O})}{\partial t} \tag{1b}$$

$$\frac{\partial}{\partial x}\left(\rho_W \frac{k\,Kr_W}{\mu_W}\frac{\partial p_W}{\partial x}\omega_{w-W}\right) = \varphi\frac{\partial(\rho_W s_W \omega_{w-W})}{\partial t} \quad (1c)$$

$$\frac{\partial}{\partial x}\left(\rho_W \frac{k\,Kr_W}{\mu_W}\frac{\partial p_W}{\partial x}\omega_{CO_2-W}\right) - U = \varphi\frac{\partial(\rho_W s_W \omega_{CO_2-W})}{\partial t} \quad (1d)$$

123

124 Eq. (1a) and Eq (1b) are respectively based on the oil and CO_2 component balance in the
125 oil phase, which is a mixture of oil and CO_2 components. Eq. (1c) and Eq (1d) are,
126 respectively, based on water and CO_2 component balance in the water phase, which is a
127 mixture of water and CO_2 components. $\omega_{I-\alpha}$ shows the mass fraction of component 'I' (oil,
128 water or CO_2) in phase 'α' (oil or water). The notation used for oil and water components are
129 small letters of 'o' and 'w' while for the oil and water phases are capital letters of 'O' and
130 'W' respectively. p_α, ρ_α and s_α are the pressure, the mass density and the saturation of phase
131 'α', respectively. The difference between phase pressures is capillary pressure (p_c) as shown
132 below.

$$p_c = p_O - p_W = f(s_W) \quad (2a)$$

133

134 The following auxiliary equations also need to be solved together with the above PDEs:
135

$$\sum s_\alpha = 1 \qquad \alpha\text{: oil, water phase} \quad (2b)$$

$$\sum \omega_{I-\alpha} = 1 \qquad \text{I: oil, water or } co_2 \text{ components} \quad (2c)$$

136 The 'U' (g/ cm^3/ sec) parameter is added to Eqs. (1b) and (1d) to control and capture the
137 migration of CO_2 from water into the oil. 'U' shows the grams of CO_2 displacing between
138 phases per unit volume at a period of time of 't'. The driving force for CO_2 migration is the
139 CO_2 concentration difference in water and oil phases as formulated below:

$$U = K \times \left(\rho_W \times \omega_{CO_2-W} \times k_{eq} - \rho_O \times \omega_{CO_2-O}\right) = K \times \left(k_{eq} C_{CO_2-W} - C_{CO_2-O}\right) \quad (3)$$

140 where C_{CO_2-O} is CO_2 concentration in the oil phase and C_{CO_2-W} is the CO_2 concentration
141 in the water phase. k_{eq} is the distribution or partition coefficient that captures how CO_2 is

distributed between the phases at the equilibrium state. It is a measure of the difference in solubility of the CO_2 component in oil and water phases, and is defined as the ratio of CO_2 concentration in oil and water phases at the equilibrium state. k_{eq} is defined to be: $k_{eq}=\frac{C_{CO_2-O}^*}{C_{CO_2-W}^*}$, where $C_{CO_2-O}^*$ and $C_{CO_2-W}^*$ are the equilibrium CO_2 concentrations in oil and water, respectively [30]. Eq. (3) shows that the CO_2 is transferred until its concentration in the phases reaches equilibrium. In the above equation, the K parameter has the unit of 'sec^{-1},' and it controls the rate at which the CO_2 is transferred. It acts similar to the mass transfer coefficient (MTC) and is referred to as MTC. The MTC value is considered as a lumped interphase mass transfer parameter here, but it is dependent on overall microscopic mass transfer coefficient and the specific interfacial area, that is the oil-water interfacial area per unit volume [29]. This approach is widely used in the literature by researchers in hydrology [31, 22, 23, 25]. The MTC is determined by history matching of production data here. It is worth mentioning that, contrary to the model here, in conventional compositional approach that is used for example by ECLPSE300, CO_2 is partitioned between the oil and water phases based on the equilibrium concentration at each simulation time step using the fugacity equilibration method. For more details, the Manual of ECLIPSE software can be checked (ECLIPSE Software Manual 2015) [32]. We previously simulated and studied a WI and its corresponding CWI coreflood experiment using the developed model. In the experiment chosen for study, the core was fully saturated with normal decane (n-decane) at 2000 psi and 38 ^{0}C. Table 1 shows the core properties.

Table 1: The core properties [10].

Core	Length (cm)	Diameter (cm)	Porosity (fraction)	Pore Volume (cm^3)	Permeability (mD)
Sandstone Clashach (water-wet)	33.2	4.986	0.19	123.16	1300

First, WI experiment was simulated and production data including total oil production(TOP) and differential pressure across the core (DP) were history matched using genetic algorithm. The details of the simulation can be found in [2]. Figure 1 and Figure 2 show the relative permeability (Kr) and capillary pressure (p_c) curves obtained by history matching of the production data.

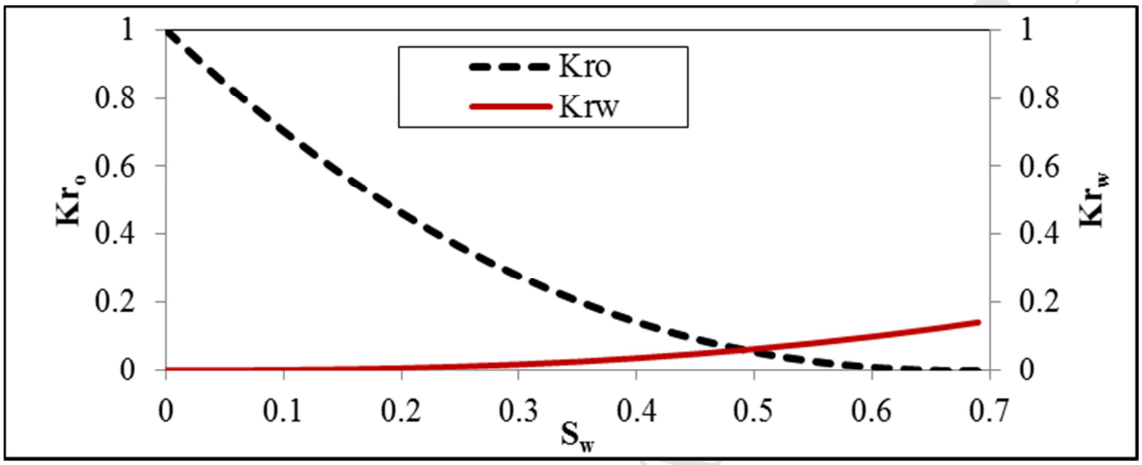

Figure 1. Relative permeability curve, WI experiment.

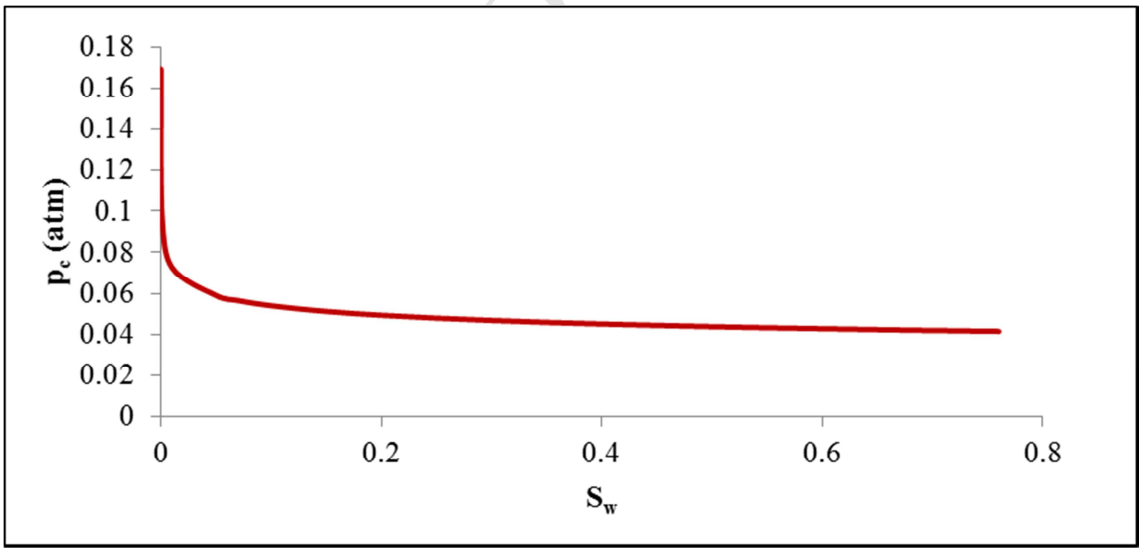

Figure 2. Capillary pressure curve, WI experiment.

Next CWI experiment was simulated. The unknown MTC parameter was tuned to history match the production of CWI experiment. The tuned MTC value obtained was 5×10^{-7} sec^{-1}. The E300 compositional simulator was also used to simulate CWI. The goal was to compare the results from our non-equilibrium based model with an equilibrium based software. In

E300 model, the specific KEYWORD of CO2SOL was used. The CO2SOL KEYWORD allows CO_2 to be present within the three phases of oil, gas and water while other components can be in the oil and gas phases. In other words, the CO2SOL option allows CO_2 to be dissolved in water phase. In ECLIPSE, water is allowed to be present as a separate aqueous phase only. The equality of CO_2 fugacity in oil and gas phases is used to calculate the CO_2 distribution between the gas and oil phases. Densities and fugacities of oil and gas phase are calculated using the tuned Peng-Robinson cubic equation of state (EOS)[33, 34]. Aqueous phase properties and the amount of CO_2 dissolved in water are computed using solubility data available in the ECLIPSE software [32](ECLIPSE Software Manual 2015). It should be mentioned that using the CO2SOL option, it is not allowed to have CO_2 content in the injected water. Therefore, we had to define two injection wells at the same place, where one was to inject CO_2 and the other to inject water. The individual injection rate of each well was adjusted to have a net injection rate of 20 cm^3/hr of carbonated water with 5% wt CO_2 content. Figure 3 compares the CWI recovery factor (RF) profile predicted by E300 with those from our tuned model and also from the experiment.

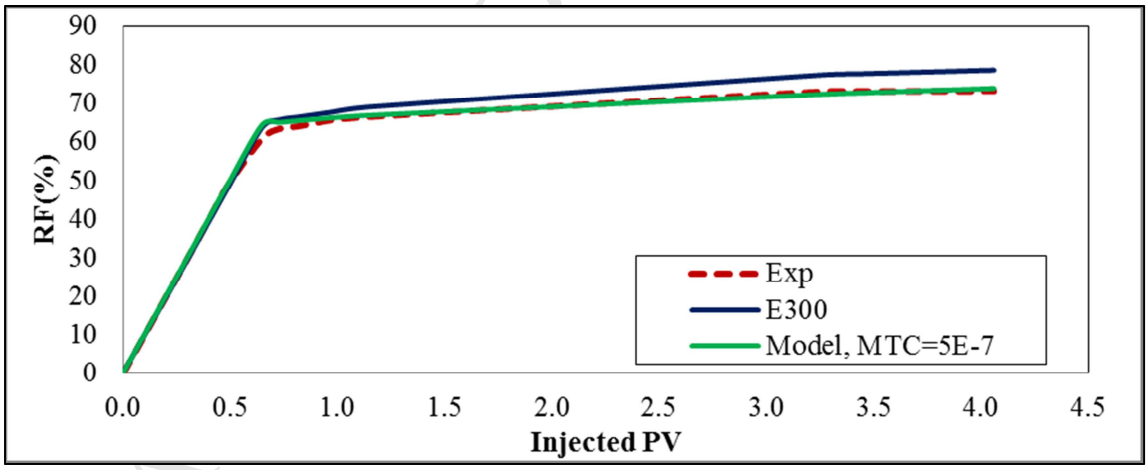

Figure 3. Comparison of CWI-RF profile predicted by E300 with those from our model and experiment.

As it can be observed in Figure 3, E300 has over predicted the recovery factor (RF) due to the equilibrium assumption made by E300 that allows more CO_2 transfer to the oil phase at a specific period of time. This comparison shows that, the CO_2 distribution between the phases

during this CWI has not reached the equilibrium state. Moreover, we can infer that, the MTC value has to be greater than that obtained by tuning of experimental data i.e., greater than 5×10^{-7} sec^{-1} (tune-MTC), otherwise, the system cannot reach the equilibrium state. To check this, the tune-MTC was increased in our model by a factor of 3 and it was observed that the prediction of our model and that by E300 became the same as shown in Figure 4.

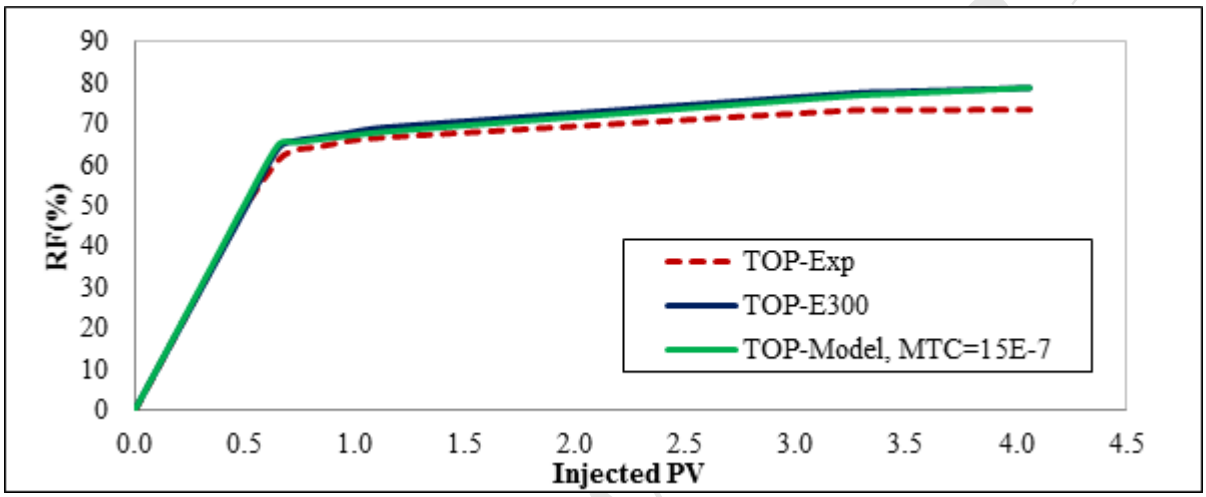

Figure 4. Comparison of CWI-RF profile predicted by E300 with those from our model at large MTC value of 15×10^{-7} and also from the experiment.

It can be inferred from Figure 4 that with having a faster mass transfer, the equilibrium state can be reached. In other words, the actual MTC i.e., the tune-MTC (5×10^{-7} sec^{-1}) obtained for the coreflood experiment investigated here, is three times smaller than of the MTC value required to reach the equilibrium state i.e., the equilibrium-MTC (15×10^{-7} sec^{-1}). Based on the above discussion, it is evident that it will be helpful if we can find an index to identify the situation needed to reach the equilibrium during CWI processes. To achieve this, it is required to find the parameters which affect the equilibrium condition during CWI process in the core. It was shown above that if the MTC value is increased by a factor of 3, the system can reach the equilibrium state. However, it should be noted that MTC is a basic characteristic of the fluid and core used in the study. It is expected that for a fixed fluid system, the MTC value should be different for different cores with different pore geometries

and heterogeneities. This is because at the pore-scale level (in microscopic view), pore geometry and heterogeneity will affect the fluid distribution in the core and in turn will influence the interface area between the phases which is an important parameter in mass transfer process. As a result, the value of MTC cannot be changed naturally for a specific system as it is an inherent characteristic of the system. In the following section, by analyzing the results of a comprehensive sensitivity analysis, a dimensionless number is defined to identify the conditions needed to reach the equilibrium state considering the MTC is a fixed intrinsic parameter of the system.

3. RESULTS AND DISCUSSIONS

3.1. Equilibrium Dimensionless Number (N_e)

To quantify the contribution of the mass transfer during the simulation of the CWI process, a dimensionless number was developed. To do so, a sensitivity analysis was performed using the coreflood experimental data presented above. The core properties (i.e. core length and diameter, porosity and permeability) as well as the injection rate (operational condition) were changed, and based on these changes; the MTC was adjusted such that our model could produce the same results as those of E300. In other words, we identified the MTC values that maintain full equilibrium when core properties were changed in a base-case. It should be noted that in the base-case (equilibrium-case), the injection rate and the core properties were the same as the original values but the equilibrium-MTC value of 15×10^{-7} sec^{-1} was used to have the same results from both the model and E300. The tune-case (actual non-equilibrium case) was also considered which relates to the case when the tune-MTC (i.e. 5×10^{-7}) was used by our simulator to match the experimental data. It has to be added that the tune-MTC is the actual MTC and the equilibrium-MTC is the one that makes the local equilibrium condition to be valid. As will be discussed later, this equilibrium condition can be

achieved more realistically by altering the core properties or injection rate. The difference between the tune-case and the base-case is the value of MTC. It should be noted that this exercise was carried out for carbonated water-decane fluid system; therefore, the effect of fluid properties was excluded. Table 2 shows the results of this sensitivity analysis. It demonstrates different combinations of core properties and injection rates (seven cases in total) at which the output of E300 and our model are the same. That is, injection rate and core properties were changed from the corresponding base values in case-2 and MTCs were adjusted such that the results of our model and E300 became the same. The profile of oil recovery was used to compare the results. It should be noted that in all cases of 2-7, the same recovery factor profile was predicted by both E300 and our model.

Table 2: Combination of core properties and operational condition when the same result by the E300 and the developed simulators is obtained for CWI coreflood experiment.

Case No.		Injection rate (cm^3/sec)	MTC (sec^{-1})	Area (A) (cm^2)	Length (L) (cm)	k (mD)	φ (fraction)
1	Tune-case (Non-equilibrium case)	0.0055	5×10^{-7}	19.5	33.2	1300	0.19
2	Base-case (Equilibrium case)	0.0055	15×10^{-7}	19.5	33.2	1300	0.19
3	Effect of injection rate	0.002 ($\frac{1}{3}\times0.0055$)	5×10^{-7} ($\frac{1}{3}\times15\times10^{-7}$)	19.5	33.2	1300	0.19
4	Effect of core length	0.0055	30×10^{-7} ($2\times15\times10^{-7}$)	19.5	16.6 ($\frac{1}{2}\times33.2$)	1300	0.19
5	Effect of core cross section area	0.0055	30×10^{-7} ($2\times15\times10^{-7}$)	9.75 ($\frac{1}{2}\times19.5$)	33.2	1300	0.19
6	Effect of core permeability	0.0055	15×10^{-7} ($1\times15\times10^{-7}$)	19.5	33.2	650 ($\frac{1}{2}\times1300$)	0.19
7	Effect of core porosity	0.0055	15×10^{-7} ($1\times15\times10^{-7}$)	19.5	33.2	1300	0.095 ($\frac{1}{2}\times0.19$)

In Table 2, case-3 to case-7 are benchmarked against case-2. The red color in case-3 to case-7 shows a different value as compared to its corresponding value in case-2. For example, Table 2 shows that, when the injection rate is decreased by a factor of three as shown in case-3, the MTC needs to also be decreased by a factor of three from its base value in our model to produce the same result as case-2. It should be noted that RF factor predicted by E300 was not changed by changing the injection rate while our simulator predicted higher RF at lower injection rates. Moreover, when the length of the core is reduced by half, the MTC needs to be increased by a factor of two (comparing case-2 and case-4). Furthermore, when the cross sectional area of the core is decreased by a factor of two (i.e. the core diameter is decreased by a factor of $\sqrt{2}$), the MTC needs to be increased by a factor of two(comparing case-2 and case-5). However, the mass transfer rate is not affected by the porosity and the permeability of the core (comparing case-2 with case-6 and case-7). This exercise shows that the effect of mass transfer can be compensated by the parameters which control the resident time of the fluids inside the core. That is, when the core length is increased or when the velocity of fluids in the core are decreased (by decreasing injection rate or increasing the core cross sectional area), the fluids have more time to exchange the CO_2 causing the system to reach the equilibrium state. In other words, if the interphase mass transfer rate is low but the resident time of the fluids inside the system is large enough, the equilibrium state can be achieved. Using the results of this sensitivity exercise (shown in Table 2), a dimensionless number so-called equilibrium number (N_e) can be defined and introduced as follows:

$$N_e = \frac{L \times MTC}{u} = \frac{L \times MTC \times A}{q_{inj}} \quad (4)$$

where u is the superficial velocity obtained by the injection rate (q_{inj}) divided by the core cross sectional area (A), L is the core length and MTC is the lumped interphase mass transfer

coefficient. This dimensionless number is the product of resident time (L/u) and MTC values that characterizes the degree of non-equilibrium by comparing the mass transfer time scale and the convective flow time scale. Similar dimensionless numbers can be found in the literature. For example, Damköhler number shows the reaction timescale relative the convection flow time scale [35, 36] in reactive flow systems. In addition, Damköhler number is also used by a few researchers to show the importance of mass transfer relative to convective flow in porous media, however the resident time is not included making it different from the above suggested number[21]. Table 3 shows the equilibrium number calculated for different combinations of core properties and operational conditions presented in Table 2.

Table 3: Equilibrium number for different combinations of core properties and injection rates when the same results by the E300 and the developed simulators is obtained for the CWI coreflood experiment.

Case No.		Injection rate (cm^3/sec)	MTC (sec^{-1})	Area (A) (cm^2)	Length (L) (cm)	N_e
1	Tune-case (Non-equilibrium case)	0.0055	5×10^{-7}	19.5	33.2	0.06
2	Base-case (Equilibrium case)	0.0055	15×10^{-7}	19.5	33.2	0.17
3	Effect of injection rate	0.002 ($\frac{1}{3}\times0.0055$)	5×10^{-7} ($\frac{1}{3}\times15\times10^{-7}$)	19.5	33.2	0.17
4	Effect of core length	0.0055	30×10^{-7} ($2\times15\times10^{-7}$)	19.5	16.6 ($\frac{1}{2}\times33.2$)	0.17
5	Effect of core cross section area	0.0055	30×10^{-7} ($2\times15\times10^{-7}$)	9.75 ($\frac{1}{2}\times19.5$)	33.2	0.17

It can be seen that in all cases, N_e is equal to 0.17 (~ 0.2). However, N_e is 0.06 for the tune-case (non-equilibrium case, case-1) at which the equilibrium assumption is not valid and E300 over predicted the recovery factor compared to those predicted by our model. It should be noted that the pore level properties such as wettability or interfacial area are inherently captured by MTC lumped-parameter. Table 3 shows that for this specific coreflood system

the equilibrium number is the same for the all cases that have reached equilibrium state. It should be noted that for all the equilibrium cases, the same recovery factor is predicted by our model and E300. In line with this, for the base-case (case-2) in Table 3, the MTC value is 3 times higher than the tune-MTC value. However, if all parameters are the same as that of the tune-case, E300 cannot be used to simulate the CWI process as it will over predict the production data. However, if N_e can be increased by a factor of 3, i.e. from 0.058 to 0.175, E300 can be used to simulate CWI as it will produce similar results as those by our model. That is, if the N_e value is 0.2 or higher it can be said that the amount of CO_2 being transferred between the phases is such that the local equilibrium assumption used by the E300 is acceptable.

To increase the N_e value, MTC cannot be changed as it is a natural characteristic of the core and fluids used during the coreflood experiment. For example, for the coreflood experiment discussed above, MTC is a fixed value that was obtained by tuning production data (tune-MTC). Therefore, for a fixed MTC value, the injection rate can be reduced or core length can be increased to assure that the simulation performed based on the local equilibrium assumption, is acceptable. Hence, for this specific coreflood experiment, if a new CWI experiment is designed so that the original injection rate is decreased by three times or using a core plug with a length three times longer than the original core length, it can be said that E300 can be used to simulate it with acceptable accuracy.

3.2. Reservoir-scale Simulation

To check the validity of the N_e constraint explained above for the equilibrium state, it is worth comparing the prediction of E300 and our model for a large-scale setup. This will help to discover if the results of our model and E300 are consistent at reservoir-scale. It seems that for a large-scale model where oil and water have enough time to exchange the CO_2, the

equilibrium assumption can be valid. To investigate this, a large synthetic 1-D model was created using the same fluid and rock data as those from the above discussed coreflood experiment. We can study a 1-D model because our simulator is based on one-dimensional flow. The dimensions of the model were selected to be 1500 ft ×10 ft ×10 ft and was only discretized in the 'x' direction. As the dimension in the 'x' direction is very large relative to the dimensions in the 'y' and 'z' directions, it can be assumed that the flow is one-dimensional. Figure 5 shows the front view of the model with injection and production wells.

Figure 5. The front view of the model.

The injection well was operated under a constant injection rate while the production well was controlled by a constant bottom-hole pressure. The operational conditions (i.e. the constraints) of the wells were chosen to mimic the operational conditions used during the coreflood experiments and also to maintain the local equilibrium conditions. In other words, we need to have similar conditions for the reservoir model as those of the coreflood experiment in terms of equilibrium situation and also active forces. Under similar conditions that can be controlled through N_e and also capillary number (N_c) values, we are able to use the core-scale MTC discussed above (i.e., tune-MTC) at a large-scale whilst maintaining the equilibrium conditions. Therefore, the capillary number (N_c) is also considered to have a similar N_c value at both core- and reservoir-scale. Capillary number represents the ratio of viscous to capillary forces [37, 38] and is defined as follows [39-41]:

$$N_c = \frac{u\mu}{\varphi\sigma} = \frac{q_{inj}\mu}{\varphi\sigma A} \quad (5)$$

where u and μ are the velocity and viscosity of displacing fluid, respectively. σ is the interfacial tension between displacing (carbonated water here) and displaced fluid (n-decane here). Table 4 shows the values needed for calculation of N_c in the experiment.

Table 4: The capillary number calculated for the coreflood experiment.

q_{inj} (m^3/day)	Area (A) (m^2)	μ_w (kg/m.sec)	σ^* (N/m)	φ	u (q_{inj}/A) (m/day)	N_c (Eq.5)
480×10^{-6}	19.5×10^{-4}	0.66×10^{-3}	20×10^{-3}	0.19	0.25	5×10^{-7}

*: estimated from [42] for carbonated water-decane at reservoir conditions.

As calculated in Table 4, N_c is 5×10^{-7} which is in the range of typical capillary dominated flow observed during reservoir-scale water flooding projects[39, 40]. The injection rate should be selected to meet the criteria imposed by capillary and equilibrium numbers. Table 5 shows the maximum injection rate which can be used in order to satisfy the constraints imposed by capillary and equilibrium numbers.

Table 5: Injection rate obtained based on the constraints imposed by equilibrium and capillary numbers.

N_e	N_c	MTC (sec^{-1})	cross section area (ft^2)	L (ft)	Maximum injection rate based on N_c (Rbbl/d)	Maximum injection rate based on N_e (Rbbl/d)
0.2	5×10^{-7}	5×10^{-7}	100	1500	14.6	5771

Table 5 shows that we can inject carbonated water with a high rate of 5771 Rbbl/day without violating the equilibrium criterion imposed by the N_e value. That is, if the injection rate is equal or smaller than 5771 Rbbl/day, N_e will be equal or greater than 0.2 when the

tune-MTC is used. This is because for a large-scale model, even though the inherent interphase mass transfer rate that is controlled by MTC value might be low, but the fluids still have enough contact time for mass exchange. Moreover, due to the size of the model, even at high injection rates, the resident time of fluid inside the reservoirs is long enough to reach the local equilibrium state. On the other hand, to have a similar capillary dominated flow at this large-scale, based on N_c criterion, the maximum injection rate that can be used is 14.6 Rbbl/day. It should be noted that in this example the cross sectional area was small because we were forced to make a 1-D model. This resulted in the small injection rate calculated based on N_c value. If the cross sectional area was larger, a larger rate could be estimated based on the N_c criterion (based on Eq. 5), and a very large injection rate based on N_e criterion (based on Eq. 4). It is worth mentioning that, in real 3-D reservoir models, as the cross sectional area is large, a large value for injection rate can be used assuring both criteria of N_c and N_e are met. That is, the equilibrium state is not a concern at large-scale. In this example, the injection rate should be smaller than 14.6 (based on N_c criteria) and 5771 Rbbl/day (based on N_e criteria). An injection rate 6.77 Rbbl/day was selected such that the interstitial velocity is 2 ft/day as the typical velocity of fluids in reservoirs[43]. Our model was used to simulate both WI and CWI for this large-scale setup. However, first a sensitivity analysis was performed to select the optimum number of the gridblocks. CWI is simulated during this sensitivity experiment because, a finer grid size is expected for CWI due to the presence of CO_2. The numbers of grids (Nx) were increased from 5 to 30. It was observed that increasing the grid numbers above 10 does not have a considerable effect on RF predicted by our model. Based on this sensitivity analysis, to be on the safe side, the model was discretized and divided into 30 gridblocks in ‘x’ direction each with a length of 50 ft (i.e., 30 × 50 ft=1500 ft).

Figure 6 compares the RF of the WI predicted by E300 and by our model in black-oil mode. It can be observed that they have generated similar results. This shows the good performance of the developed model for a large-scale case. Next the CWI was simulated. It was explained above that for a large-scale model, the assumption of local equilibrium should be valid. This was discussed when the equilibrium number was introduced and investigated. Therefore, it is expected that our model and E300 result in the same RF if the original tune-MTC value (i.e. 5×10^{-7} sec^{-1}) was used.

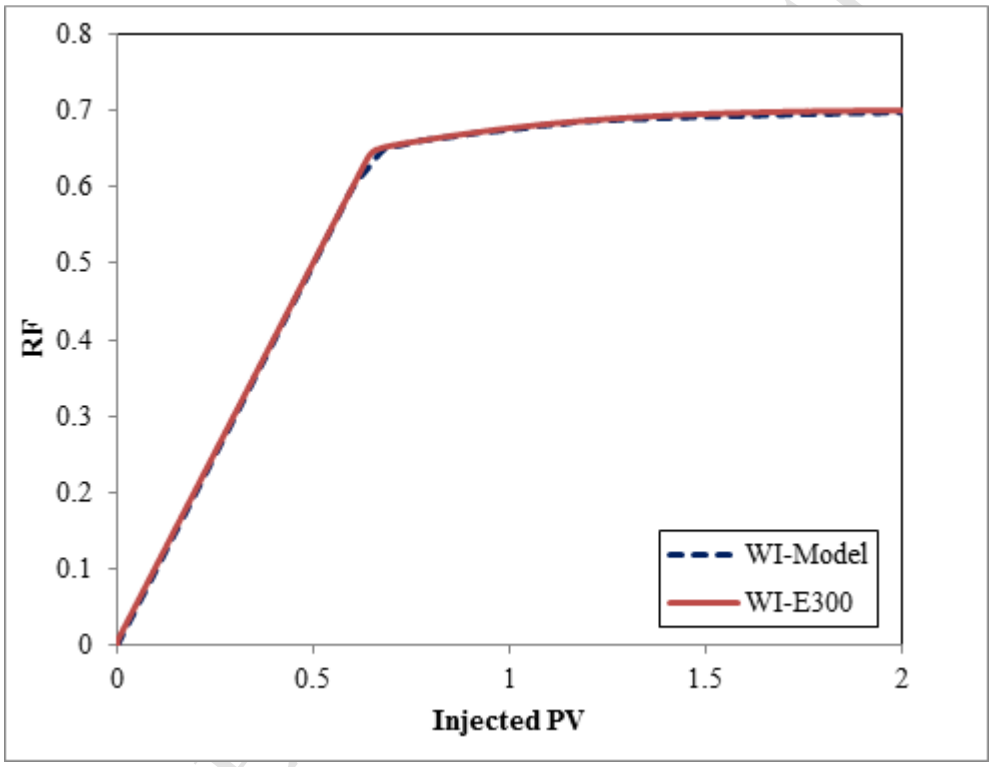

Figure 6. RF of the WI predicted by E00 compared to that by our model.

Figure 7 compares the RF of the CWI predicted by E300 and by our model. It can be observed that the results predicted by these two different simulators are similar. This experiment was repeated using the higher injection rate of 14.6 Rbbl/day. Both our simulator and E300 predicted the same recovery factor profile as that obtained for 6.77 Rbb/day case.

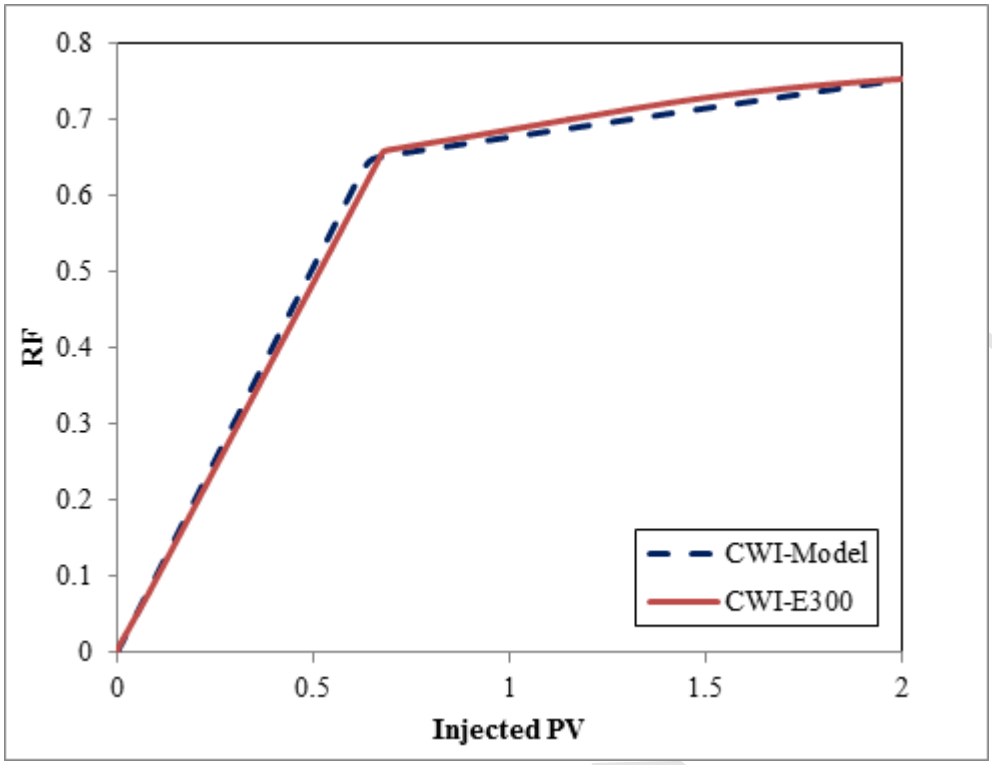

Figure. 7. RF of the CWI predicted by E00 compared to that by our model.

This example demonstrates that if the CO_2 has enough time to be transferred into the oil phase, it can reach its equilibrium concentration as captured in these simulations. However, it is important to run more simulations and investigate different cases to further support these results. It is worth mentioning that in our core-scale study, we did not have the effect of gravity (as the core had been positioned horizontally during the experiment) and heterogeneity (as the core was homogeneous) and accordingly we did not include them in the large-scale model discussed above. In other words, we wanted to compare two similar systems with the only difference in capturing the mass transfer mechanisms.

3.3. CO_2 Storage

CO_2 will be stored in the system as a dissolved component in remaining oil and water (solubility trapping). Figure 8 shows the CO_2 storage curves predicted by the core-scale and reservoir-scale models. The plot shows the ratio of total volume of CO_2 stored relative to total

volume of CO_2 injected versus the pore volume of injected carbonated water. It can be observed that at reservoir-scale, more volume of CO_2 can be stored. It is expected, because at large-scale, CO_2 has enough time to be transferred to oil phase before being produced from the production well. In other words, if the system cannot reach the equilibrium state during CWI process, less volume of CO_2 will be stored in the formation.

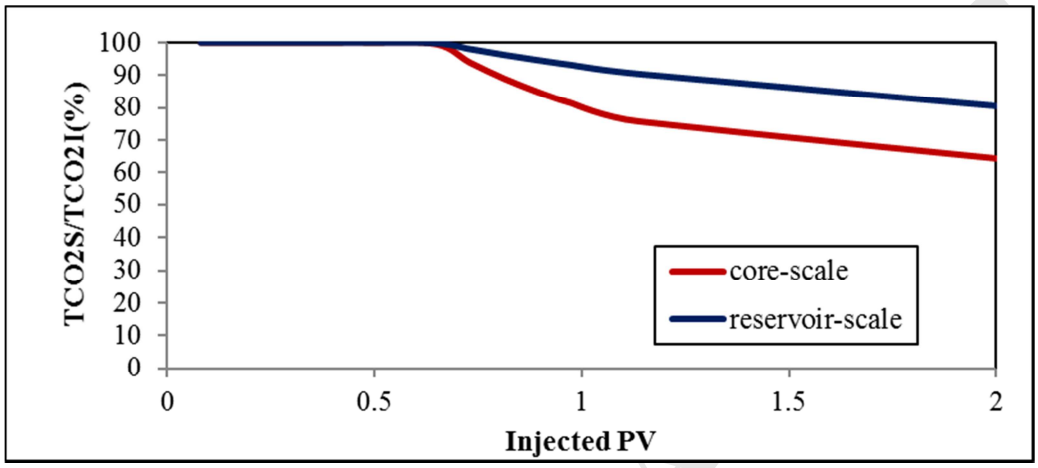

Figure. 8. CO_2 storage curves predicted by core-scale and reservoir- scale models.

4. SUMMARY AND CONCLUSIONS

In this study, the simulation of the CWI process was investigated in core-scale and also in reservoir-scale using our non-equilibrium based model as well as the equilibrium based ECLIPSE 300 (E300) simulator. A new dimensionless number, i.e. equilibrium number (N_e), was introduced by performing a sensitivity analysis using the core-scale simulation results. It was shown that during the coreflood experiments, N_e is constant and within a specific range of N_e, it can be assumed that the equilibrium state will be reached during CWI. A synthetic one-dimensional reservoir-scale setup was then created to meet the criteria imposed by the capillary and equilibrium numbers. The data of coreflood experiment (rock and fluid data, Kr and pc curves) were used for this reservoir-scale system. The setup was used to simulate a WI and its corresponding CWI using both our model and E300. The goal was to investigate the

performance of our model for large-scale setups. The RF predicted by E300 were the same as those predicted by our model for both WI and CWI cases. This exercise showed that for the large-scale model, the criterion imposed by N_e value was met as a result of the reservoir size and the assumption of equilibrium was valid. In other words, it can be explained that for CWI at reservoir-scale, there is enough time for CO_2 to be transferred and distributed between oil and water phases based on its equilibrium concentration. As a result, available compositional simulators such as E300 can be used for simulation of CWI at reservoir-scale. In addition, as a result of equilibrium, higher oil recovery factor and CO_2 storage were obtained for the reservoir-scale model compared to those from the core-scale model.

Nomenclatures

$\omega_{I-\alpha}$: Mass fraction of component 'I' (oil, water or CO_2) in phase 'α' (oil or water).

$C_{CO_2-\alpha}$: CO_2 concentration (g/cm^3) in phase 'α' (oil or water).

$C_{CO_2-\alpha}{}^*$: CO_2 concentration (g/cm^3) in phase 'α' (oil or water) at the equilibrium state.

k_{eq} : Distribution coefficient, here is 9.6.

MTC: Pseudo inter-phase mass transfer coefficient (MTC) (sec^{-1}).

p : phase pressure (atm).

s: phase saturation.

φ : porosity.

k: absolute permeability (mD).

A: cross sectional area.

q_{inj}: injection rate.

Acknowledgments

This work was a part of 'carbonated water injection' joint industry project (JIP) performed at Heriot-Watt University. This JIP was sponsored equally by Total, Petrobras, Abu Dhabi

Company for Onshore Oil Operations (ADCO), BG Group, UK Department of Energy & Climate Change (DECC) and Galp Energia that is gratefully acknowledged.

APENDIX: NUMERICAL SOLUTION TECHNIQUE

The four coupled governing equations together with the associated boundary and initial conditions were solved simultaneously for pressure, saturation and mass fractions as the main dependent variables, using the finite difference technique. The fully implicit solution technique was used to solve the governing equations for the variables of p_O, s_W, ω_{o-O} and ω_{CO_2-W}.

Substituting Eqs. (2a) to (2c) in Eqs. (1a) to (1d) and discretizing the equations will give:

$$\varphi\Delta_t[\rho_O\,(1\text{-}s_W)\,\omega_{o-O}]=\Delta_x[\rho_O\,\omega_{o-O}\;\lambda_O\,\Delta_x p_O] \tag{1-A}$$

$$\varphi\Delta_t[\rho_O\,(1\text{-}s_W)\,(1\text{-}\omega_{o-O})]=\Delta_x[\rho_O\,(1\text{-}\omega_{o-O})\,\lambda_o\,\Delta_x p_O]+U \tag{2-A}$$

$$\varphi\Delta_t[\rho_W\,s_W\,(1\text{-}\omega_{CO_2-W})]=\Delta_x[\rho_w\,(1\text{-}\omega_{CO_2-W})\,\lambda_w\,\Delta_x(p_O\text{-}p_c)] \tag{3-A}$$

$$\varphi\Delta_t[\rho_W\,s_W\,\omega_{CO_2-W}]=\Delta_x[\rho_W\,\omega_{CO_2-W}\,\lambda_W\,\Delta_x(p_O\text{-}p_c)]\text{-}U \tag{4-A}$$

where $\lambda_O=\frac{k\,Kr_O}{\mu_O}$, $\lambda_W=\frac{k\,Kr_W}{\mu_W}$, $\Delta_x[\,]=\frac{\Delta[\,]}{\Delta x}$ and $\Delta_t[\,]=\frac{\Delta[\,]}{\Delta t}$. The equations can be written in the following residual forms:

$$R_{o\text{-}O}^{n+1}=\Delta_x[\rho_O\,\omega_{o-O}\;\lambda_O\,\Delta_x p_O]^{n+1}\text{-}\varphi\Delta_t[\rho_O\,(1\text{-}s_W)\,\omega_{o-O}] \tag{5-A}$$

$$R_{co_2\text{-}O}^{n+1}=\Delta_x\left[\rho_O\,(1\text{-}\omega_{o-O})\,\lambda_o\,\Delta_x p_O\right]^{n+1}+U^{n+1}\text{-}\varphi\Delta_t[\rho_O\,(1\text{-}s_W)\,(1\text{-}\omega_{o-O})] \tag{6-A}$$

$$R_{w\text{-}W}^{n+1}=\Delta_x[\rho_w\,(1\text{-}\omega_{CO_2-W})\,\lambda_w\,\Delta_x(p_O\text{-}p_c)]^{n+1}\text{-}\varphi\Delta_t[\rho_W\,s_W\,(1\text{-}\omega_{CO_2-W})] \tag{7-A}$$

$$R_{co_2\text{-}W}^{n+1}=\Delta_x\left[\rho_W\,\omega_{CO_2-W}\,\lambda_W\,\Delta_x(p_O\text{-}p_c)\right]^{n+1}\text{-}U^{n+1}\text{-}\varphi\Delta_t\left[\rho_W\,s_W\,\omega_{CO_2-W}\right] \quad (8\text{-A})$$

where $R_{I-\alpha}$ is the residual value of each equation written for component I in phase α. 'n+1' shows that the calculation is performed at the new time step (i.e. implicit solution). The residual values of each equation should be zero that is achieved by employing the Newton-Raphson iterative method (Eq. 9-A).

$$X_{itr+1}^{n+1}=X_{itr}^{n+1}\text{-}\frac{R_{I-\alpha}^{n+1}(X_{itr}^{n+1})}{\frac{\partial R_{I-\alpha}^{n+1}(X_{itr}^{n+1})}{\partial X_{itr}^{n+1}}} \quad \text{or} \quad J_R(X_{itr}^{n+1})(X_{itr+1}^{n+1}\text{-}X_{itr}^{n+1}) = -R_{I-\alpha}^{n+1}(X_{itr}^{n+1}) \quad (9\text{-A})$$

where 'itr' is the iteration number and 'X' is the vector of dependent variables ($X = [p_O, s_W, \omega_{o-O}, \omega_{CO_2-W}]$. $J_R(X_{itr}^{n+1})$ is the Jacobin matrix (or derivative matrix) of residual values which its components are $\frac{\partial R_{I-\alpha}^{n+1}(X_{itr}^{n+1})}{\partial X_{itr}^{n+1}}$ [44, 45].

References

[1] J. Foroozesh, M. Jamiolahmady, Simulation of carbonated water injection coreflood experiments: An insight into the wettability effect, Fuel, 184 (2016) 581-589.

[2] J. Foroozesh, M. Jamiolahmady, M. Sohrabi, Mathematical modeling of carbonated water injection for EOR and CO_2 storage with a focus on mass transfer kinetics, Fuel, 174 (2016) 325-332.

[3] M. Sohrabi, N.I. Kechut, M. Riazi, M. Jamiolahmady, S. Ireland, G. Robertson, Safe storage of CO_2 together with improved oil recovery by CO_2-enriched water injection, Chemical Engineering Research and Design, 89 (2011) 1865-1872.

[4] M. Riazi, M. Sohrabi, M. Jamiolahmady, Experimental study of pore-scale mechanisms of carbonated water injection, Transport in porous media, 86 (2011) 73-86.

[5] M. Sohrabi, M. Riazi, M. Jamiolahmady, N.I. Kechut, S. Ireland, G. Robertson, Carbonated water injection (CWI)-a productive way of using CO_2 for oil recovery and CO_2 storage, Energy Procedia, 4 (2011) 2192-2199.

[6] M.A. Ahmadi, M. Zeinali Hasanvand, S. Shokrollahzadeh Behbahani, A. Nourmohammad, A. Vahidi, M. Amiri, G. Ahmadi, Effect of operational parameters on the performance of carbonated water injection: Experimental and numerical modeling study, The Journal of Supercritical Fluids, 107 (2016) 542-548.

[7] A.H. Alizadeh, M. Khishvand, M.A. Ioannidis, M. Piri, Multi-scale experimental study of carbonated water injection: An effective process for mobilization and recovery of trapped oil, Fuel, 132 (2014) 219–235.

[8] A. Fathollahi, B. Rostami, Carbonated water injection: Effects of silica nanoparticles and operating pressure, The Canadian Journal of Chemical Engineering, 93 (2015) 1949–1956.

[9] N.I. Kechut, M. Jamiolahmady, M. Sohrabi, Numerical simulation of experimental carbonated water injection (CWI) for improved oil recovery and CO_2 storage, Journal of Petroleum Science and Engineering, 77 (2011) 111-120.
[10] M. Sohrabi, N.I. Kechut, M. Riazi, M. Jamiolahmady, S. Ireland, G. Robertson, Coreflooding studies to investigate the potential of carbonated water injection as an injection strategy for improved oil recovery and CO_2 storage, Transport in porous media, 91 (2012) 101-121.
[11] Y. Dong, B. Dindoruk, C. Ishizawa, E.J. Lewis, An experimental investigation of carbonated water flooding, in: SPE Annual Technical Conference and Exhibition (SPE No. 145380), Denver, Colorado, USA 2011.
[12] N. Mosavat, F. Torabi, Performance of secondary carbonated water injection in light oil systems, Industrial & Engineering Chemistry Research, 53 (2013) 1262-1273.
[13] H. Li, S. Zheng, D. Yang, Enhanced Swelling Effect and Viscosity Reduction of Solvent(s)/CO_2/Heavy-Oil Systems, SPE Journal, 18 (2013) 695-707.
[14] H. Emami-Meybodi, H. Hassanzadeh, C.P. Green, J. Ennis-King, Convective dissolution of CO in saline aquifers: Progress in modeling and experiments, International Journal of Greenhouse Gas Control, 40 (2015) 238-266.
[15] J.L. Shelton, J.C. McIntosh, A.G. Hunt, T.L. Beebe, A.D. Parker, P.D. Warwick, R.M. Drake, J.E. McCray, Determining CO_2 storage potential during miscible CO_2 enhanced oil recovery: Noble gas and stable isotope tracers, International Journal of Greenhouse Gas Control, 51 (2016) 239-253.
[16] J. Foroozesh, M. Jamiolahmady, M. Sohrabi, S. Ireland, Non-equilibrium based compositional simulation of carbonated water injection EOR technique, in: ECMOR XIV-14th European Conference on the Mathematics of Oil Recovery, EAGE, Sicily, Italy, 2014.
[17] Y.-B. Chang, B.K. Coats, J.S. Nolen, A compositional model for CO_2 floods including CO_2 solubility in water, SPE Reservoir Evaluation & Engineering, 1 (1998) 155-160
[18] S. Embid, O. Rivas, Simulation of Miscible Displacement with Interphase Mass Transfer Resistance, SPE Advanced Technology Series, 2 (1994) 161-168.
[19] W. Wu, P. Wang, M. Delshad, C. Wang, G.A. Pope, M.M. Sharma, Modeling Non-Equilibrium Mass Transfer Effects for a Gas Condensate Field, in: SPE Asia Pacific Conference on Integrated Modelling for Asset Management, Society of Petroleum Engineers, Kuala Lumpur, Malaysia, 1998.
[20] Anwar, A.H.M. F., Estimation of mass transfer coefficients using air-liquid interfacial area in porous media, Journal of Environmental Research and Technology, 3 (2008) 331-341.
[21] J. Cho, M.D. Annable, P. Rao, Measured Mass Transfer Coefficients in Porous Media Using Specific Interfacial Area, Environmental Science & Technology, 39 (2005) 7883-7888.
[22] S.E. Powers, L.M. Abriola, J.W.J. Weber, An experimental investigation of nonaqueous phase liquid dissolution in saturated subsurface systems: steady state mass transfer rates, Water Resources Research Journal, 28 (1992) 2691-2705.
[23] S.E. Powers, L.M. Abriola, J.W.J. Weber, An experimental investigation of nonaqueous phase liquid dissolution in saturated subsurface systems: transient mass transfer rates, Water Resources Research, 30 (1994) 321-332.
[24] S.E. Powers, C.O. Loureiro, L.M. Abriola, W.J. Weber, Theoretical study of the significance of nonequilibrium dissolution of nonaqueous phase liquids in subsurface systems, Water Resources Research, 27 (1991) 463-477.
[25] H. Yoon, J.H. Kim, H.M. Liljestrand, J. Khim, Effect of water content on transient nonequilibrium NAPL–gas mass transfer during soil vapor extraction,, Journal of Contaminat Hydrology, 54 (2002) 1–18.
[26] D. Zhou, F.J. Fayers, F.M. Orr Jr., Scaling of multiphase flow in simple heterogeneous porous media, SPE Reservoir Engineering, 12 (1997) 173–178.

[27] D.J. Wood, R.T. Johns, V. Nunez, A Screening Model for CO2 Flooding and Storage in Gulf Coast Reservoirs Based on Dimensionless Groups, SPE Reservoir Evaluation & Engineering, 11 (2008) 513-520.
[28] L. Li, S. Khorsandi, R.T. Johns, R.M. Dilmore, CO_2 enhanced oil recovery and storage using a gravity-enhanced process, International Journal of Greenhouse Gas Control, 42 (2015) 502-515.
[29] J. Geller, J. Hunt, Mass transfer from nonaqueous phase organic liquids in water-saturated porous media, Water resources research, 29 (1993) 833-845.
[30] A. Leo, C. Hansch, D. Elkins, Partition coefficients and their uses, Chemical Reviews, 71 (1971) 525-616.
[31] P.T. Imhoff, P.R. Jaffe, Effect of liquid distribution on gas-water phase mass transfer in an unsaturated sand during infiltration, Contaminat Hydrology, 16 (1994) 359-380.
[32] ECLIPSE Simulation Software Manual 2015, in: Schlumberger (Ed.).
[33] H. Nourozieh, M. Kariznovi, J. Abedi, Measurement and correlation of saturated liquid properties and gas solubility for decane, tetradecane and their binary mixtures saturated with carbon dioxide, Fluid Phase Equilibria, 337 (2013) 246-254.
[34] C.L. Yaws, Chemical properties handbook, McGraw-Hill, New York, 2014.
[35] S.H. Fogler, Elements of Chemical Reaction Engineering (4th Edition) Prentice Hall, 2006.
[36] W. Yanto Wijaya, S. Kawasaki, H. Watanabe, K. Okazaki, Damköhler number as a descriptive parameter in methanol steam reforming and its integration with absorption heat pump system, Applied Energy, 94 (2012) 141-147.
[37] R. Chandler, J. Koplik, K. Lerman, J.F. Willemsen, Capillary displacement and percolation in porous media, Journal of Fluid Mechanic, 119 (1982) 249-267.
[38] F.A.L. Dullien, Porous Media: Fluid Transport and Pore Structure, second ed., Academic Press, 1992.
[39] W.R. Foster, A low tension waterflooding process, Journal of Petroleum Technology, 25 (1973) 205-210.
[40] J.C. Melrose, C.F. Brandner, Role of capillary forces in determining micro-scopic displacement efficiency for oil recovery by waterflooding, Journal of Canadian Petroleum Technology, 13 (1974) 54–62.
[41] D. Tiab, E.C. Donaldson, Petrophysics: Theory and Practice of Measuring Reservoir Rock and Fluid Transport Properties, Gulf Publishing Co., Houston, Texas, 1996.
[42] A. Georgiadis, G. Maitland, J.P. Martin Trusler, A. Bismarck, Interfacial tension measurements of the (H2O+n-Decane + CO2) ternary system at elevated pressures and temperatures, Journal of Chemical &Engineering Data, 56 (2011) 4900-4908.
[43] A.L. Chen, A.C. Wood, Rate effects on water–oil relative permeability, in: International Symposium of the Society of Core Analysts, Edinburgh, Scotland, 2001.
[44] Kh. Aziz, A. Settari, Petroleum Reservoir Simulation, Applied Science Publishers, 1979.
[45] J.R. Fanchi, Principles of Applied Reservoir Simulation, Gulf Professional Publishing, Houston, USA, 2005.

- Mass transfer effect during core and reservoir scales simulation of carbonated water injection (CWI) process is investigated.
- A dimensionless number is introduced that describes the criteria needed to reach the equilibrium state during CWI process.
- Contrary to core-scale simulation, CWI can be simulated at reservoir-scale assuming instantaneous equilibrium state.